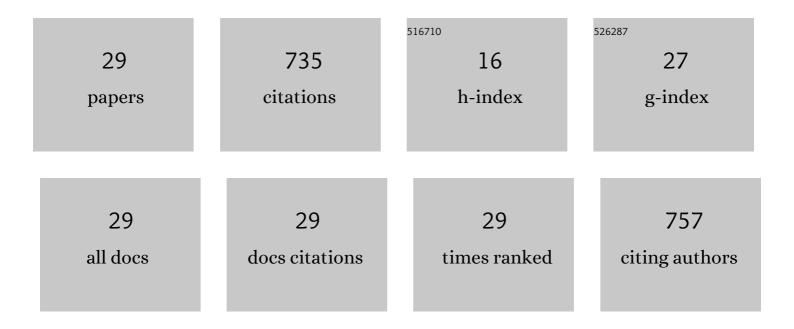


List of Publications by Year in descending order

Source: https://exaly.com/author-pdf/1747247/publications.pdf Version: 2024-02-01



DENCLI

#	Article	IF	CITATIONS
1	High speed spectral domain optical coherence tomography for retinal imaging at 500,000 Aâ€ʻlines per second. Biomedical Optics Express, 2011, 2, 2770.	2.9	106
2	Pulsatile motion of the trabecular meshwork in healthy human subjects quantified by phase-sensitive optical coherence tomography. Biomedical Optics Express, 2013, 4, 2051.	2.9	76
3	Phase-sensitive optical coherence tomography characterization of pulse-induced trabecular meshwork displacement in <i>ex vivo</i> nonhuman primate eyes. Journal of Biomedical Optics, 2012, 17, 0760261.	2.6	56
4	In vivo microstructural and microvascular imaging of the human corneo-scleral limbus using optical coherence tomography. Biomedical Optics Express, 2011, 2, 3109.	2.9	49
5	High-resolution 1050 nm spectral domain retinal optical coherence tomography at 120 kHz A-scan rate with 61 mm imaging depth. Biomedical Optics Express, 2013, 4, 245.	2.9	42
6	Extended imaging depth to 12Âmm for 1050-nm spectral domain optical coherence tomography for imaging the whole anterior segment of the human eye at 120-kHz A-scan rate. Journal of Biomedical Optics, 2013, 18, 016012.	2.6	38
7	Assessment of strain and strain rate in embryonic chick heartin vivousing tissue Doppler optical coherence tomography. Physics in Medicine and Biology, 2011, 56, 7081-7092.	3.0	35
8	Statistical analysis of motion contrast in optical coherence tomography angiography. Journal of Biomedical Optics, 2015, 20, 116004.	2.6	35
9	Optical microangiography provides an ability to monitor responses of cerebral microcirculation to hypoxia and hyperoxia in mice. Journal of Biomedical Optics, 2011, 16, 096019.	2.6	34
10	Full anterior segment biometry with extended imaging range spectral domain optical coherence tomography at 1340Ânm. Journal of Biomedical Optics, 2014, 19, 1.	2.6	34
11	SNR-Adaptive OCT Angiography Enabled by Statistical Characterization of Intensity and Decorrelation With Multi-Variate Time Series Model. IEEE Transactions on Medical Imaging, 2019, 38, 2695-2704.	8.9	30
12	Orthogonal dispersive spectral-domain optical coherence tomography. Optics Express, 2014, 22, 10081.	3.4	22
13	Measurement of Strain and Strain Rate in Embryonic Chick Heart In Vivo Using Spectral Domain Optical Coherence Tomography. IEEE Transactions on Biomedical Engineering, 2011, 58, 2333-2338.	4.2	21
14	<i>In vivo</i> functional imaging of blood flow and wall strain rate in outflow tract of embryonic chick heart using ultrafast spectral domain optical coherence tomography. Journal of Biomedical Optics, 2012, 17, 0960061.	2.6	19
15	Improved motion contrast and processing efficiency in OCT angiography using complex-correlation algorithm. Journal of Optics (United Kingdom), 2016, 18, 025301.	2.2	18
16	Responses of Peripheral Blood Flow to Acute Hypoxia and Hyperoxia as Measured by Optical Microangiography. PLoS ONE, 2011, 6, e26802.	2.5	18
17	Improvement of Decorrelation-Based OCT Angiography by an Adaptive Spatial-Temporal Kernel in Monitoring Stimulus-Evoked Hemodynamic Responses. IEEE Transactions on Medical Imaging, 2020, 39, 4286-4296.	8.9	12
18	High performance OCTA enabled by combining features of shape, intensity, and complex decorrelation. Optics Letters, 2021, 46, 368.	3.3	12

Peng Li

#	Article	IF	CITATIONS
19	ID-OCTA: OCT angiography based on inverse SNR and decorrelation features. Journal of Innovative Optical Health Sciences, 2021, 14, .	1.0	12
20	Visualization of the ocular pulse in the anterior chamber of the mouse eye <i>in vivo</i> using phase-sensitive optical coherence tomography. Journal of Biomedical Optics, 2014, 19, 090502.	2.6	10
21	High-speed high-precision and ultralong-range complex spectral domain dimensional metrology. Optics Express, 2015, 23, 11013.	3.4	10
22	Anterior Segment Biometry with Phenylephrine and Tropicamide during Accommodation Imaged with Ultralong Scan Depth Optical Coherence Tomography. Journal of Ophthalmology, 2019, 2019, 1-5.	1.3	9
23	Noninvasive OCT angiography-based blood attenuation measurements correlate with blood glucose level in the mouse retina. Biomedical Optics Express, 2021, 12, 4680.	2.9	7
24	Anterior segment optical coherence tomography evaluation of ocular graft-versus-host disease: a case study. Quantitative Imaging in Medicine and Surgery, 2015, 5, 163-70.	2.0	6
25	Pulsatile motion of trabecular meshwork in a patient with iris cyst by phase-sensitive optical coherence tomography: a case report. Quantitative Imaging in Medicine and Surgery, 2015, 5, 171-3.	2.0	6
26	Dynamic inverse SNR-decorrelation OCT angiography with GPU acceleration. Biomedical Optics Express, 2022, 13, 3615.	2.9	6
27	Correlation of optical attenuation coefficient estimated using optical coherence tomography with changes in astrocytes and neurons in a chronic photothrombosis stroke model. Biomedical Optics Express, 2019, 10, 6258.	2.9	5
28	Assessment of Full-Eye Response to Osmotic Stress in Mouse Model In Vivo Using Optical Coherence Tomography. Journal of Ophthalmology, 2015, 2015, 1-8.	1.3	4
29	Swept source intraoperative OCT angiography. Journal of Innovative Optical Health Sciences, 2021, 14, 2140009.	1.0	3